

Protracted screening in the periodic Anderson model

A. N. Tahvildar-Zadeh and M. Jarrell

Department of Physics, University of Cincinnati, Cincinnati, Ohio 45221

J. K. Freericks

Department of Physics, Georgetown University, Washington, DC 20057-0995

(Received 24 September 1996)

The asymmetric infinite-dimensional periodic Anderson model is examined with a quantum Monte Carlo simulation. For small conduction band filling, we find a severe reduction in the Kondo scale, compared to the impurity value, as well as protracted spin screening consistent with some recent controversial photoemission experiments. The Kondo screening drives a ferromagnetic transition when the conduction band is quarter filled and both the Ruderman-Kittel-Kasuya-Yosida (RKKY) and superexchange favor antiferromagnetism. We also find RKKY-driven ferromagnetic and antiferromagnetic transitions. [S0163-1829(97)51906-0]

INTRODUCTION

Kondo lattice materials, stoichiometric systems generally with U or Ce atoms in the valence shell, have been studied intensely over the last few decades. They display a wide variety of behaviors including the well-known transport anomalies associated with a strongly enhanced electronic mass, as well as magnetic (antiferromagnetic, incommensurate, and ferromagnetic), paramagnetic, and superconducting ground states.¹ The magnetic nature of the ground state is determined by the strength of the hybridization between the f electrons with the delocalized band states.² If the hybridization is small, then the Ruderman-Kittel-Kasuya-Yosida (RKKY) exchange dominates and the ground state is magnetic. If the hybridization is large, then either the Kondo screening removes the f moments, or charge fluctuations delocalize the f electrons destroying their moments, and the ground state is usually a Pauli paramagnet.

The periodic Anderson model (PAM) is thought to describe this competition between screening and magnetism in these materials. Both it and the single impurity Anderson model (SIAM) have been extensively studied; nevertheless, the detailed nature of the orbitally nondegenerate PAM phase diagram as well as the differences in the Kondo screening between the two models are unknown. We present exact calculations for the asymmetric PAM in infinite dimensions. We find antiferromagnetic, ferromagnetic, and paramagnetic ground states, depending upon conduction band filling n_d and model parameters. In the paramagnetic state, we find that the temperature dependence of the Kondo screening retains the same qualitative features as the SIAM, whereas the *quantitative features are quite different*. Specifically, when $n_d \ll n_f$ ($n_d \approx n_f = 1$) the Kondo scale is strongly suppressed (enhanced) and the temperature dependence of the screening is protracted (contracted) compared to the SIAM. These differences between the PAM and SIAM cannot be removed by rescaling and may provide insight into recent controversial photoemission experiments.³

The PAM Hamiltonian on a D -dimensional hypercubic lattice is

$$H = \frac{-t^*}{2\sqrt{D}} \sum_{(ij)\sigma} (d_{i\sigma}^\dagger d_{j\sigma} + \text{H.c.}) + \sum_{i\sigma} (\epsilon_d d_{i\sigma}^\dagger d_{i\sigma} + \epsilon_f f_{i\sigma}^\dagger f_{i\sigma}) + V \sum_{i\sigma} (d_{i\sigma}^\dagger f_{i\sigma} + \text{H.c.}) + \sum_i U (n_{f_i\uparrow} - 1/2)(n_{f_i\downarrow} - 1/2). \quad (1)$$

In Eq. (1), $d(f)_{i\sigma}^\dagger$ destroys (creates) a $d(f)$ -electron with spin σ on site i . The hopping is restricted to the nearest neighbors and scaled as $t = t^*/2\sqrt{D}$ (we choose $t^* = 1$, the width of the Gaussian density of states, as the energy scale). U is the screened on-site Coulomb repulsion for the localized f states and V is the hybridization between d and f states. This model retains the complications of the impurity problem, including moment formation and screening but is further complicated by interactions between the moments due to RKKY and superexchange mechanisms.

FORMALISM

We use the method proposed by Metzner and Vollhardt⁴ to determine an exact solution to the interacting lattice problem. They observed that the irreducible self-energy and vertex functions become purely local as the coordination number of the lattice increases. As a consequence, the solution of this interacting lattice model may be mapped onto the solution of a local correlated impurity coupled to an effective bath that is self-consistently determined.⁵ Further details can be found in the above references and recent reviews.⁶

We employ the quantum Monte Carlo (QMC) algorithm of Hirsch and Fye⁷ to solve the remaining impurity problem. In order to model the Ce-based Kondo lattice materials, we place the correlated f band below the Fermi level (so $n_f \approx 1$) and adjust the conduction band filling by varying the Fermi level. Thus, beginning at $\beta = 10$, we choose ϵ_f and ϵ_d so that $n_f = 1$ and n_d assumes a chosen value. When the temperature is changed, we keep $\epsilon_f - \epsilon_d$ fixed and vary the chemical potential to conserve the *total* number of electrons. For the results presented here, the variation of n_f from one is less than a few percent, and the statistical error bars are less

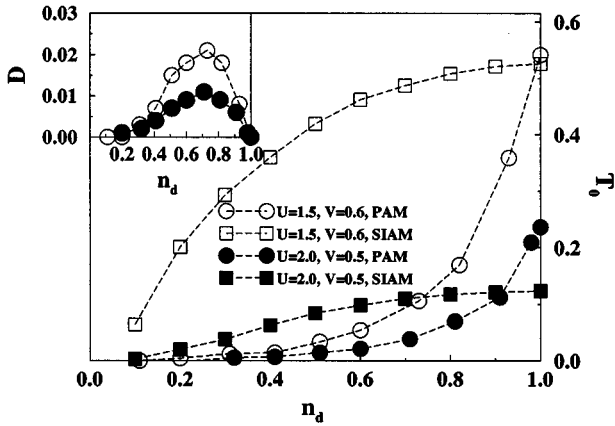


FIG. 1. Kondo temperature vs d -band filling for the infinite-dimensional PAM and SIAM at fixed half-filled f band ($n_f \approx 1.0$) and two different sets of model parameters. The inset shows the corresponding Drude weight for the PAM.

than 7%. Note that our results are symmetric under $n_d \rightarrow 2 - n_d$, and that the PAM becomes more correlated for small values of n_d and $2 - n_d$.

RESULTS

Figure 1 shows the Kondo scale for the PAM and the SIAM versus d band filling when the f band is half filled. The Kondo scales are obtained by extrapolation $\chi_{imp}(T \rightarrow 0) = 1/T_0$, where $\chi_{imp}(T)$ is the additional local susceptibility due to the introduction of the effective impurity into a host of d electrons.⁸ We see that at the symmetric limit ($n_f = n_d = 1$) the Kondo scale for the PAM is enhanced compared to the Kondo scale of the SIAM as has been found earlier.^{9,8} However, far from the symmetric limit the Kondo scale for the PAM is strongly *suppressed*.

The main consequence of this suppression is that the temperature dependence of the screening in the PAM is quite different from that of the SIAM. This is shown in Fig. 2 where the screened local f -moments $T\chi_{ff}$ for both models

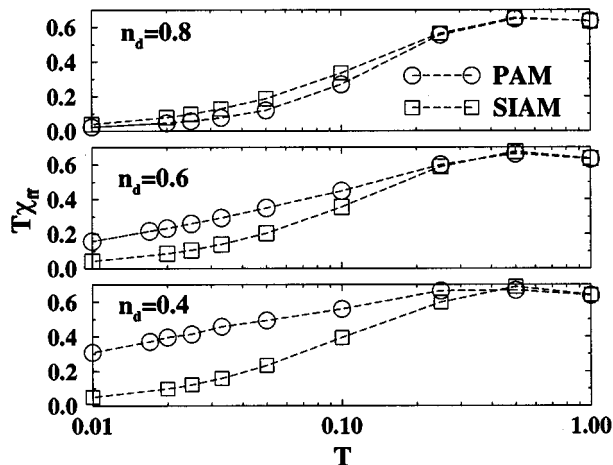


FIG. 2. The f -band magnetic moments for the PAM and the SIAM vs temperature for three different values of d -band filling when $U = 1.5$ and $V = 0.6$.

are plotted versus temperature. As expected from the impurity problem, $T\chi_{ff}$ displays a log-linear T dependence in some temperature interval. However, concomitant with the differences in T_0 , the screening of the PAM and the SIAM local moments are quite different: for most values of n_d these two curves *cannot be made to overlap by rescaling their temperature dependencies* (nor is it possible, in the PAM case, to make the curves for different d fillings overlap by rescaling T). At high temperatures, the screened local moments are identical for the PAM and the SIAM, and as the temperature is lowered below T_{0SIAM} the screening begins; however, if $n_d \ll n_f$ ($n_d \approx n_f = 1$), the screening is significantly protracted (contracted) in temperature for the PAM compared to that in the SIAM. (The contracted screening region, as well as the enhancement of the Kondo scale, when $n_d = n_f = 1$, depends strongly upon the correlation energy U , and diminishes when U is small; e.g., when $U = 1.5$, $V = 0.6$). This behavior is consistent with recent controversial photoemission experiments on single crystals of Ce-based heavy-fermion compounds, where the temperature dependence of the spectral weight in the screening peak is much less than what is expected for the SIAM.³

The Drude weight, D , calculated by extrapolation of the current-current correlation function,¹⁰ is shown in the inset to Fig. 1. For all of the data shown in Fig. 1, D is quite small and the effective electron mass (not shown) is large $m^*/m = 1/Z \geq 15$, where Z is the quasiparticle renormalization factor. In the symmetric limit, where a gap opens in the single-particle density of states, we have $D = Z = 0$. However, consistent with what is seen in the Kondo scale for the PAM, D and Z also become small when $n_d \ll 1$. When the d filling falls, there are no longer enough d electrons to completely screen the f moments. Thus, T_0 falls quickly as the d band is doped away from half filling. If this process continues, the d band becomes depopulated, and then only acts as a hopping path between the f levels. In the limit, $n_d \rightarrow 0$, the PAM may be mapped onto a strongly correlated symmetric Hubbard model¹¹ (with an on-site correlation U and a strongly reduced hopping), which is known to open a gap in the single-particle density of states and have $Z = 0$ and $D = 0$.⁶ Thus, when $n_d = 0$ or $n_d = 1$, we find that both the f and the d band densities of states vanish at the Fermi surface. However, for all other values of n_d explored, the f and d density of states remain finite (with the f density of states (DOS) only moderately enhanced) indicating that the system remains metallic.

It is clear from the Drude weight shown in the inset to Fig. 1, that the unscreened moments have a dramatic effect on the Fermi-liquid properties of the system. This may also be seen by examining the electronic distribution function $n(\epsilon_k) = T \sum_n [G^{dd}(\epsilon_k, i\omega_n) + G^{ff}(\epsilon_k, i\omega_n)]$, where G^{dd} and G^{ff} are the fully dressed d - and f -band Green's functions calculated with the QMC. $dn(\epsilon_k)/d\epsilon_k$ is calculated by numerically evaluating the derivative of the above sum. This has a peak located at the Fermi energy. The width of this peak at low temperatures (shown in Fig. 3) gives an estimate of the single-particle scattering rate, which must go to zero if a Fermi liquid is to form. This appears to happen when $n_d = 0.8, 0.6$, and 0.4 ; however, for $n_d = 0.2$, it is not clear whether a Fermi liquid forms. When $n_d \lesssim 0.4$, there is a protracted region in T of strong spin-flip scattering, beginning at

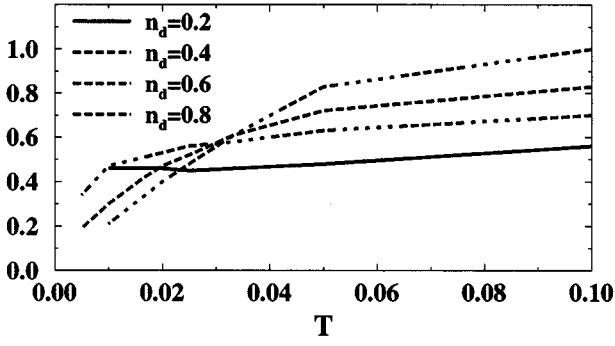


FIG. 3. Half-width of the derivative of the total occupation number, $dn(\epsilon_k)/d\epsilon_k$, at low temperatures when $U=1.5$ and $V=0.6$. In a Fermi liquid this quantity should be proportional to ZT . Any residual value represents the scattering rate at the Fermi surface. The flat slope of $w(T)$ at low temperatures for the low-filling case suggests that the Fermi liquid does not begin to form before the ferromagnetic transition (cf. Fig. 4).

$T \geq T_{0SIAM}$, and extending down to very low temperatures.

However, due to magnetic ordering for $n_d \leq 0.6$, we find no compelling evidence for non-Fermi liquid (paramagnetic) ground states. Figure 4 shows the magnetic phase diagram of the half-filled f -band PAM. T_c is obtained by extrapolating or interpolating the magnetic susceptibility assuming the mean-field form $\chi \propto 1/(T - T_c)$. There are two well-known exchange mechanisms that are usually responsible for the formation of these magnetic ground states. (i) the superexchange which results from the exchange of the local f electrons via the hybridization with the d band; this exchange always favors antiferromagnetic order of the half-filled f band and becomes strongly suppressed as the d band is filled towards $n_d = 1$;¹² (ii) the RKKY exchange which results from the scattering of a d electron from two f moments; this exchange varies (in sign and magnitude) as a function of the d -band filling.^{12,13} The inset to Fig. 4 shows the difference between the staggered and uniform RKKY exchange,

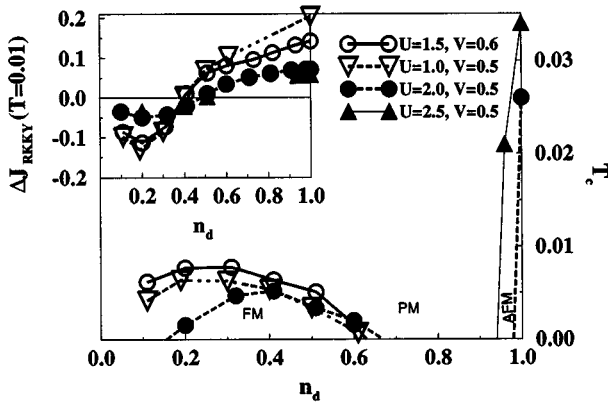


FIG. 4. Magnetic phase diagram for infinite-dimensional PAM at fixed half-filled f band ($n_f \approx 1.0$) and four different sets of model parameters. FM, PM, and AFM stand for ferromagnetic, paramagnetic, and antiferromagnetic phases, respectively. (The FM transition points for $U=2.5$, $V=0.5$ are not shown.) The inset shows the difference between the staggered and uniform RKKY exchange constants vs d -band filling.

$\Delta J_{RKKY} = J_{RKKY}(\mathbf{q}=\mathbf{Q}) - J_{RKKY}(\mathbf{q}=\mathbf{0})$, where \mathbf{Q} is the wave vector corresponding to the corner of the first Brillouin zone and

$$J_{RKKY}(\mathbf{q}) = -\frac{T}{2N} J_{fd}^2 \sum_{n,\mathbf{k}} \mathbf{G}^{dd}(\mathbf{k}, i\omega_n) G^{dd}(\mathbf{k}+\mathbf{q}, i\omega_n). \quad (2)$$

Here, $J_{fd} = -8V^2/U$, is the effective exchange between the f and d bands.¹⁴ ΔJ_{RKKY} would be proportional to the energy gained by the formation of a ferromagnet versus an antiferromagnet in the f band if RKKY were the only exchange mechanism present.

In the symmetric limit, $n_f = n_d = 1$, for the more strongly correlated model (larger U), there is an instability towards antiferromagnetism as expected from the sign of the RKKY exchange. (The superexchange, which always favors antiferromagnetism, is expected to be negligible in this limit¹².) For the less correlated model (smaller U) the Kondo scale is larger (Fig. 1) and the d electrons effectively screen away the local moments before a magnetic transition can occur,² so there is no antiferromagnetism in these cases.

As the d filling decreases from 1, the transition remains commensurate and T_c drops quickly to zero. However, as the system becomes more correlated, the size of this antiferromagnetic region increases. As n_d decreases further, the system remains a paramagnetic Fermi liquid until the d approaches quarter filling. Here, both the superexchange and the RKKY exchange still favor antiferromagnetism; nevertheless, the system has a ferromagnetic transition. The rather low transition temperature (compared to T_c at the symmetric limit), which is of the order of the Kondo scale, indicates that the mechanism behind this ferromagnetism might be related to the Kondo screening effect.

To see how Kondo screening can lead to a ferromagnetic exchange, assume the size of the Kondo polarization cloud is $1/k_F$ (Ref. 15) so the screening cloud is almost local. In this situation, every time a d electron hops to the neighboring d level it breaks its resonance with the local f electron and regains the lost resonance energy only if the f electron on the neighboring site has the same spin orientation and the d level is unoccupied.

This Kondo-exchange mechanism is substantiated by examining the staggered charge susceptibility of the d levels (not shown) which is strongly enhanced at low temperatures near quarter filling. Hence, each site occupied by a d electron tends to have its neighboring sites unoccupied, optimizing the above-mentioned mechanism. In addition, if the quarter-filled d electrons actually form a spin-polarized staggered charge-density wave, where the spins of the d electrons are aligned opposite to the ferromagnetically ordered f electrons, then the quasiparticle band opens a gap at the Fermi level. This lowers the kinetic energy of all the occupied d states. The quasiparticle band has to be sufficiently narrow for this ferromagnetic charge-density wave to have lower energy than the paramagnetically filled quasiparticle band (i.e., the gap must be on the order of the quasiparticle bandwidth, $\approx t^*Z \ll t^*$). Both the charge-density fluctuation effect and the associated Kondo exchange rapidly vanish away from quarter filling since the charge-density wave can no longer be commensurate and open a gap at the Fermi level. Thus,

the ferromagnetism for smaller values of n_d is due to RKKY exchange (which becomes ferromagnetic). Note that this Kondo-effect generated ferromagnetism at quarter filling is a special feature of the bipartite lattice.

Finally, we speculate that antiferromagnetism should return in the region near the empty d band, since in this limit the half-filled f -band PAM reduces to a half-filled Hubbard model¹¹ with strong antiferromagnetic superexchange.¹²

CONCLUSION

We investigate the phase diagram and screening of the asymmetric PAM in infinite dimensions. We find antiferromagnetic, ferromagnetic, and paramagnetic ground states, depending upon n_d and other model parameters. When the d band is quarter filled we find a ferromagnetic transition driven by protracted Kondo screening when the super and RKKY exchanges are antiferromagnetic. In the paramagnetic state, we find that the temperature dependence of the Kondo screening retains the same qualitative features as the SIAM, whereas the quantitative features are quite different. Specifically, when the number of conduction electrons is significantly less than the number of f electrons, we find that $T_{0PAM} \ll T_{0SIAM}$. This results in a protracted region of spin

screening extending from $T \geq T_{0SIAM}$ down to $T < T_{0PAM}$ or $T = T_c$. In this region, the temperature dependence of the screened local moment and presumably the associated features such as the screening resonance are protracted compared to those of the SIAM, which may provide insight into the temperature dependence of photoemission spectra in some Ce-based heavy-fermion lattice compounds.³ Finally, it is important to note that both the suppression of T_0 and the concomitant protracted screening disappear when the f -orbital degeneracy $N \rightarrow \infty$.¹⁶ Thus, T_{0PAM} also depends strongly upon N , so the addition of more f bands (either degenerate or crystal-field split) could partially restore an impurity like temperature dependence.

We would like to acknowledge stimulating conversations with A. Arko, J. Brinkmann, A. Chattopadhyay, D.L. Cox, M. Grioni, J. Joyce, Th. Pruschke, Q. Si, and F.C. Zhang. M.J. and A.N.T.-Z. would like to acknowledge the support of NSF Grant Nos. DMR-9406678 and DMR-9357199. J.K.F. acknowledges the support of ONR-YIP Grant No. N000149610828. Computer support was provided by the Pittsburgh Supercomputer Center (Grant No. DMR950010P and sponsored by the NSF) and the Ohio Supercomputer Center.

¹For a review, please see N. Grewe and F. Steglich, *Handbook on the Physics and Chemistry of Rare Earths*, edited by K.A. Gschneidner, Jr. and L.L. Eyring (Elsevier, Amsterdam, 1991), Vol. 14, p. 343; D.W. Hess, P.S. Riseborough, and J.L. Smith, *Encyclopedia of Applied Physics*, edited by G.L. Trigg (VCH Publishers Inc., New York, 1991), Vol. 7, p. 435. For a discussion of ferromagnetic Kondo lattice systems, see also A. Loidl *et al.*, Phys. Rev. B **46**, 9341 (1992).

²S. Doniach, Physica B&C **91B**, 231 (1977); S. Doniach, in *Valence Instabilities and Related Narrow-Band Phenomena*, edited by R. D. Parks (Plenum, New York, 1977).

³J.J. Joyce *et al.*, Phys. Rev. Lett. **68**, 236 (1992); see also J.J. Joyce *et al.*, *ibid.* **72**, 1774 (1994); and L.H. Tjeng *et al.*, *ibid.* **72**, 1775 (1994); D. Malterre *et al.*, Adv. Phys. **45**, 299 (1996).

⁴W. Metzner and D. Vollhardt, Phys. Rev. Lett. **62**, 324 (1989); see also E. Müller-Hartmann, Z. Phys. B **74**, 507 (1989).

⁵U. Brandt and C. Mielsch, Z. Phys. B **75**, 365 (1989); **79**, 295 (1990); **82**, 37 (1991); V. Janiš, *ibid.* **83**, 227(1991); C. Kim, Y. Kuramoto, and T. Kasuya, J. Phys. Soc. Jpn. **59**, 2414 (1990); V.

Janiš and D. Vollhardt, Int. J. Mod. Phys. B **6**, 713 (1992); M. Jarrell, Phys. Rev. Lett. **69**, 168 (1992); A. Georges and G. Kotliar, Phys. Rev. B **45**, 6479 (1992).

⁶Th. Pruschke, M. Jarrell, and J.K. Freericks, Adv. Phys. **42**, 187 (1995); A. Georges, G. Kotliar, W. Krauth, and M. Rozenberg, Rev. Mod. Phys. **68**, 13 (1996).

⁷J. E. Hirsch and R. M. Fye, Phys. Rev. Lett. **56**, 2521 (1989).

⁸M. Jarrell, Phys. Rev. B **51**, 7429 (1995).

⁹T. M. Rice and K. Ueda, Phys. Rev. B **34**, 6420 (1986).

¹⁰D.J. Scalapino, S. White, and S. Zhang, Phys. Rev. B **47**, 7995 (1993).

¹¹Th. Pruschke, Z. Phys. B **81**, 319 (1990).

¹²Qimiao Si, Jian Ping Lu, and K. Levin, Phys. Rev. B **45**, 4930 (1992).

¹³R. M. Fye, Phys. Rev. B **41**, 2490 (1990).

¹⁴J. R. Schrieffer and P. A. Wolff, Phys. Rev. **149**, 491 (1966).

¹⁵V. Barzykin *et al.*, Phys. Rev. Lett. **76**, 4959 (1996).

¹⁶N. Read, D.M. News, and S. Doniach, Phys. Rev. B **30**, 3841 (1984).